High mobility group box 1 enables bacterial lipids to trigger receptor-interacting protein kinase 3 (RIPK3)-mediated necroptosis and apoptosis in mice

Received for publication, December 6, 2018, and in revised form, April 4, 2019 Published, Papers in Press, April 18, 2019, DOI 10.1074/jbc.RA118.007040

Ran Meng[‡§], Lan Gu[‡¶], Yanyan Lu[‡¶], Kai Zhao[‡¶], Jianfeng Wu[‖], Haichao Wang[**], Jiahuai Han[‖], Yiting Tang[‡ ‡‡1], and Ben Lu[‡¶§§¶¶2]

*From the [‡]Department of Hematology and Key Laboratory of Non-resolving Inflammation and Tumor and the [§]Postdoctoral Research Station of Clinical Medicine, The 3rd Xiangya Hospital, Central South University, Changsha, Hunan Province 410000, China, the [¶]Key Laboratory of Medical Genetics, School of Biological Science and Technology, Central South University, Changsha, Hunan Province 410000, China, the [‖]State Key Laboratory of Cellular Stress Biology, Innovation Center for Cell Signaling Network, School of Life Sciences, Xiamen University, Xiamen, Fujian 361005, China, the **Department of Emergency Medicine, North Shore University Hospital, Northwell Health, Manhasset, New York 11030, the [‡‡]Department of Physiology, School of Basic Medical Science, Central South University, Changsha, Hunan Province 410000, China, the [§§]Key Laboratory of Sepsis Translational Medicine of Hunan, Central South University, Changsha, Hunan Province 410000, China, and the [¶¶]Department of Pathophysiology, School of Basic Medical Science, Jinan University, Guangzhou, Guangdong Province 510632, China*

Edited by Dennis R. Voelker

Receptor-interacting protein kinase 3 (RIPK3) is a key regulator of programmed cell death and inflammation during viral infection or sterile tissue injury. Whether and how bacterial infection also activates RIPK3-dependent immune responses remains poorly understood. Here we show that bacterial lipids (lipid IVa or lipid A) form a complex with high mobility group box 1 (HMGB1), released by activated immune cells or damaged tissue during bacterial infection, and that this complex triggers RIPK3- and TIR domain-containing adapter-inducing IFN-β (TRIF)-dependent immune responses. We found that these responses lead to macrophage death, interleukin (IL)-1α release, and IL-1β maturation. In an air-pouch inflammatory infiltration model, genetic deletion of *Ripk3*, *Trif*, or IL-1 receptor (*Il-1R*), or monoclonal antibody-mediated HMGB1 neutralization uniformly attenuated inflammatory responses induced by Gram-negative bacteria that release lipid IVa and lipid A. These findings uncover a previously unrecognized mechanism by which host factors and bacterial components work in concert to orchestrate immune responses.

To survive bacterial infection and promote tissue repair, the host immune system is armed with a series of pattern recognition receptors that recognize both pathogen-associated molecular patterns (PAMPs)[3] released from microbes and damage-associated molecular patterns (DAMPs) released by damaged host cells (1). Infections and anti-microbial immune responses unavoidably cause tissue damage, rendering the immune system exposed to both PAMPs and DAMPs. However, how PAMPs and DAMPs work in concert to orchestrate host immune responses remains poorly defined.

High mobility group box 1 (HMGB1) is a prototypical DAMP and an evolutionarily conserved protein virtually expressed in all type of cells. Under physiological conditions, intracellular HMGB1 functions as a nonhistone chromatin-binding protein that regulates gene expression and protects cells from oxidative stress (2, 3). During infection or tissue injury, damaged cells release HMGB1 into the extracellular space (4–6), where it regulates immune responses, cell migration, tissue regeneration, and tumorigenesis through multiple receptors such as the receptor for advanced glycation end products or TLR4 (6–18). Previous studies show that HMGB1 could enhance nucleic acid-induced immune responses (11, 14) and promote inflammatory responses through CD14 by direct binding to lipopolysaccharide (LPS) (19–21). Although exploring the role of HMGB1 in mediating PAMPs-mediated inflammation, we found that HMGB1 could also physically interact with Gram-negative bacteria-derived lipid IVa or lipid A. Both lipid IVa and lipid A are the precursor lipids for the biosynthesis of LPS that reside within the bacteria and can be released into the extracellular space when bacteria are dead. Unexpectedly, the interaction between HMGB1 and lipid IVa or lipid A enables lipid IVa

This work was supported by National Key Scientific Project Grant 2015CB910700 (to B. L.) and National Natural Science Foundation of China Grants 81422027 (to B. L.), 81400149 (to Y. T.), and 81470345 (to B. L.). The authors declare that they have no conflicts of interest with the contents of this article.

This article contains Figs. S1–S6.

[1] To whom correspondence may be addressed: Dept. of Physiology, School of Basic Medical Science, Central South University, 168 Tongzipo Rd., Changsha 410013, China. Tel.: 86-0731-88618214; Fax: 0731-88921910; E-mail: yitingtang@csu.edu.cn.

[2] To whom correspondence may be addressed: Dept. of Hematology, The 3rd Xiangya Hospital, Central South University, 138 Tongzipo Rd., Changsha 410013, China. Tel.: 86-0731-88618214; Fax: 0731-88921910; E-mail: xybenlu@csu.edu.cn.

[3] The abbreviations used are: PAMP, pathogen-associated molecular patterns; HMGB1, high mobility group box 1; RIPK3, receptor-interacting protein kinase 3; DAMP, damage-associated molecule pattern molecule; IL-1β, interleukin-1β; LPS, lipopolysaccharide; NLRP3, NLR family pyrin domain-containing 3; PKR, double-stranded RNA-dependent protein kinase; TRIF, Toll/interleukin-1R (TIR) domain-containing adapter-inducing interferon; MLKL, mixed lineage kinase domain-like; TLR4, Toll-like receptor 4; TNFα, tumor necrosis factor-α; MEF, mouse embryonic fibroblasts; PI, propidium iodide; PBMC, peripheral blood mononuclear cells; IAV, influenza A virus.

or lipid A to efficiently activate receptor-interacting protein kinase 3 (RIPK3) and trigger MLKL-dependent necroptosis as well as caspase-8 – dependent apoptosis, resulting in IL-1α release and IL-1β maturation. These responses are mediated by the TLR4-TRIF signaling, and absolutely dependent on the presence of both HMGB1 and bacterial lipid (IVa or A). In an air-pouch inflammatory infiltration model, the genetic deletion of *Ripk3*, *Trif,* or *Il-1R*, or neutralizing HMGB1 attenuates the nonresolving inflammation induced by Gram-negative bacteria. These findings uncover a previously unrecognized mechanism by which host factors and bacterial components work in concert to orchestrate RIPK3-dependent immune responses under pathophysiological conditions.

Results

HMGB1 enables lipid IVa or lipid A to trigger RIPK3-mediated necroptosis, apoptosis, and inflammation

To investigate whether HMGB1 and bacterial lipids could work in concert to orchestrate immune responses, mouse peritoneal macrophages were stimulated with lipid A or lipid IVa in the absence or presence of highly purified recombinant HMGB1 protein. Only in the presence of HMGB1 can lipid IVa or lipid A induce a marked release of LDH, IL-1α, and IL-1β (Fig. 1*A*), and an increase in the cleavage of pro-IL-1β in the WT peritoneal macrophages (Fig. 1*B*). Flow cytometry analysis revealed an increase in the percentage of cells undergoing necrosis (PI^+) and apoptosis (PI^-) after challenging mouse peritoneal macrophages with both HMGB1 and lipid IVa or lipid A (Fig. 1*C*), but not HMGB1, lipid IVa, or lipid A alone (Fig. S1). EM examination showed the occurrence of necrosis (Fig. 1*D*, *red arrows*) and apoptosis (Fig. 1*D*, *blue arrows*) in the macrophages treated with HMGB1/lipid mixtures. To confirm the importance of HMGB1 in mediating bacterial lipid action, mouse peritoneal macrophages were stimulated simultaneously with lipid IVa or lipid A in combination with necrotic cell lysate of $Hmgb1^{+/+}$ or $Hmgb1^{-/-}$ mouse embryonic fibroblasts (MEFs). Our data shown that endogenous HMGB1 released from necrotic WT MEFs enabled lipid IVa or lipid A to induce the release of IL-1α and IL-1β, which was markedly inhibited by HMGB1 neutralizing monoclonal antibodies (Fig. 1*E*, Fig. S2). To further confirm the notion in human cells, we stimulated human peripheral blood mononuclear cells (PBMC) with HMGB1 and Lipid IVa/Lipid A, and found that HMGB1 significantly enhanced the release of IL-1α and IL-1β, induced by Lipid A, but not Lipid IVa, which has been reported as an antagonist in human (Fig. S3). These observations indicate that extracellular HMGB1 could enable lipid IVa or lipid A to trigger necrosis, apoptosis, IL-1α release, and IL-1β maturation.

RIPK3 is a serine/threonine kinase that is crucial for a programmed necrosis process termed necroptosis (22–28). Although the canonical function of RIPK3 is to mediate necroptosis, RIPK3 also regulates apoptosis and other immune responses under certain circumstances (29). In response to influenza A virus (IAV) infection, RIPK3 is required for activation of the NLRP3 inflammasome, which mediates the IL-1β maturation through caspase-1 (30). RIPK3 could also promote caspase-8 – dependent IL-1β maturation and TLR4-dependent proinflammatory cytokine production (31, 32). In light of the involvement of RIPK3 in the regulation of necroptosis, apoptosis, IL-1α release, and IL-1β maturation, we next determined whether RIPK3 is required for these HMGB1/bacterial lipid–mediated responses. The deletion of *Ripk3* almost completely blocked the HMGB1/lipid IVa or HMGB1/lipid A–induced release of LDH and cytokines (IL-1α and IL-1β) (Fig. 1, *A* and *B*), and the parallel induction of apoptosis and necroptosis (Fig. 1, *C* and *D*). Furthermore, necrotic lysate of $Hmgb1^{+/+}$ MEFs failed to facilitate the lipid IVa- or lipid A-mediated IL-1α and IL-1β release from *Ripk3*-deficient macrophages (Fig. 1*E*). Together, these findings establish HMGB1 as an important regulator of bacterial lipid-mediated and RIPK3-dependent cell death and inflammatory responses.

HMGB1 binding is critical for lipid IVa and lipid A to trigger the RIPK3-dependent necroptosis, apoptosis, and inflammation

To determine whether HMGB1 could physically interact with lipid IVa or lipid A, we developed a HMGB1 lipid-binding assay (Fig. 2*A*) to quantitatively characterize the dynamics of HMGB1 binding to lipid IVa or lipid A. As shown in Fig. 2*A*, free uncoated lipid IVa or lipid A dose-dependently inhibited the anchoring of HMGB1 proteins to the lipid IVa- or lipid A-coated plate, indicating that HMGB1 is able to bind lipid IVa and lipid A. *Rhodobacter sphaeroides*-derived penta-acylated LPS (LPS-RS) is a potent LPS antagonist that has been reported to compete for the LPS-binding site on LBP (33, 34). In this study, we found that LPS-RS competitively inhibited the binding of HMGB1 to lipid IVa or lipid A (Fig. 2*B*). Furthermore, the addition of LPS-RS dose-dependently suppressed the HMGB1/lipid IVa or HMGB1/lipid A-induced IL-1α and IL-1β release from mouse macrophages (Fig. 2*C*). Consistently, LPS-RS prevented HMGB1/lipid IVa- or HMGB1/lipid A-induced necroptosis and apoptosis in mouse peritoneal macrophages (Fig. 2*D*). To further prove that HMGB1-lipid binding is important for RIPK3-mediated necroptosis, apoptosis, and inflammation, we used HPep6, a synthetic peptide that are located in the B-box domains of HMGB1 known to specifically block the HMGB1-LPS association by binding to lipid A moieties of LPS (35), and found that HPep6 also dose-dependently inhibited HMGB1 + lipid A-induced release of LDH, IL-1α, and IL-1β (Fig. 2*E*). These results suggest that HMGB1 binding is essential for lipid IVa and lipid A to trigger RIPK3-dependent necroptosis, apoptosis, and IL-1 release.

TLR4-TRIF signaling mediates bacterial lipid-induced RIPK3-dependent necroptosis, apoptosis, and inflammation in the presence of HMGB1

Next we investigated how HMGB1 enables lipid A or lipid IVa to trigger RIPK3-dependent necroptosis, apoptosis, and IL-1 release. Because HMGB1, lipid A, and lipid IVa are all capable of binding to TLR4, the deletion of TLR4 indeed completely abolished the HMGB1/lipid IVa or HMGB1/lipid A-induced release of LDH, IL-1α, IL-1β, and TNFα (Fig. 3*A*). Similarly, TLR4 deficiency also prevented the HMGB1/lipid IVa- or HMGB1/lipid A-induced apoptosis and necroptosis in mouse peritoneal macrophages (Fig. 3*B*). Moreover, necrotic lysate of $Hmgb1^{+/+}$ MEFs facilitated the lipid IVa- or lipid A-mediated

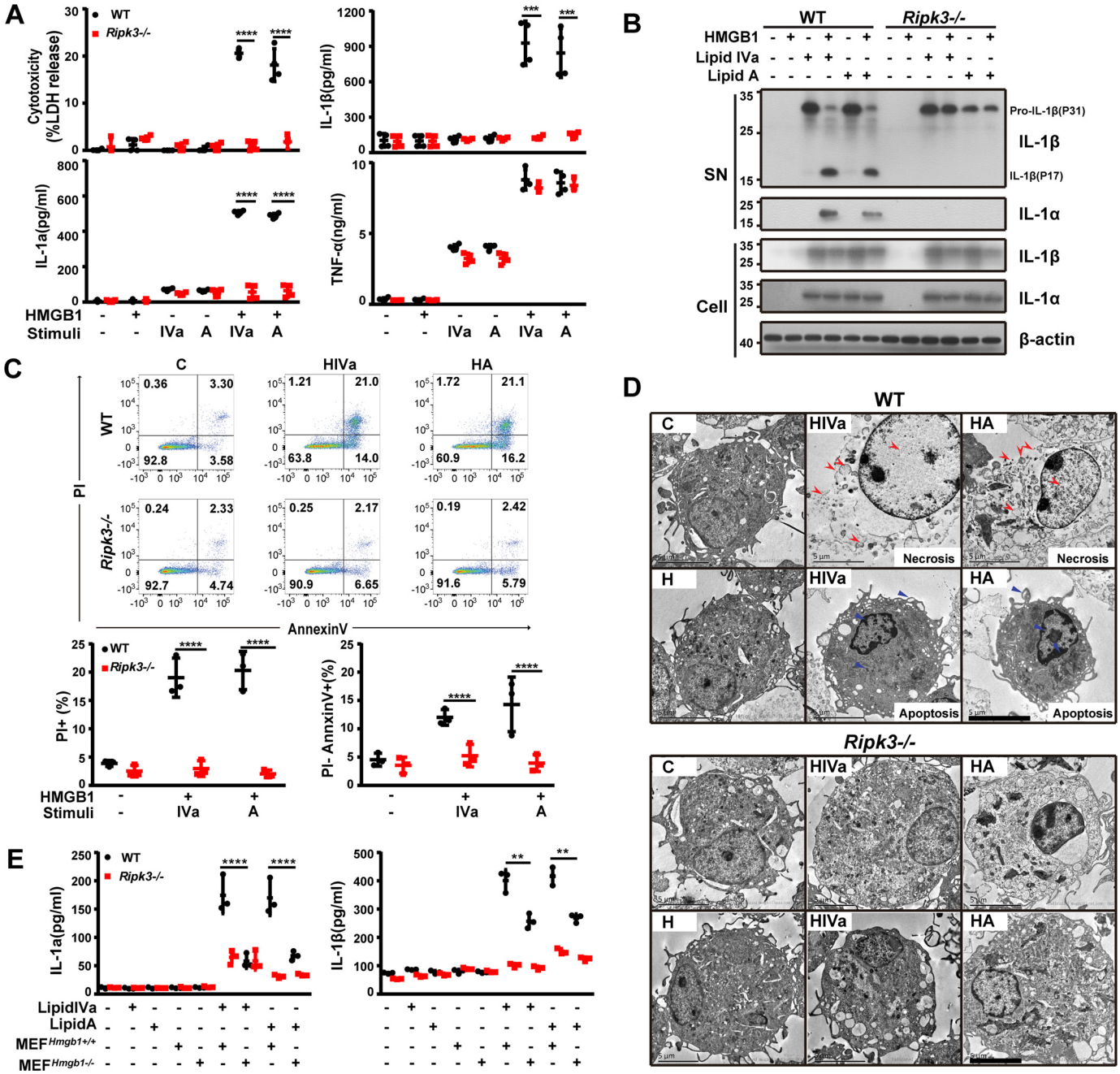

Figure 1. HMGB1 enables microbial lipids to trigger proinflammatory cell death. *A,* LDH, IL-1α, IL-1β, and TNFα measured from culture supernatants of peritoneal macrophages from wildtype (WT) and *Ripk3*$^{-/-}$ mice following stimulation with lipid IVa or lipid A (1 μg/ml) in the absence or presence of HMGB1 (0.4 μg/ml). *B,* Western blot for processed IL-1α and IL-1β released from WT and *Ripk3*$^{-/-}$ peritoneal macrophages stimulated with lipid IVa or lipid A (1 μg/ml) in the absence or presence of HMGB1 (0.4 μg/ml). *C,* flow cytometry analysis of WT or *Mlkl*$^{-/-}$ peritoneal macrophages undergoing necrosis (*PI*$^{+}$) or apoptosis (*PI*$^{-}$) of stimulation with lipid IVa or lipid A (1 μg/ml) in the presence of HMGB1 (0.4 μg/ml). *D,* the EM shows the morphology of WT and *Ripk3*$^{-/-}$ peritoneal macrophages after stimulation with HMGB1 (0.4 μg/ml) + lipid IVa or lipid A (1 μg/ml). The *red arrows* indicate the expansion of the cell volume, organelle swelling, and plasma membrane rupture. The *blue arrows* indicate intact cell membrane and condensed chromatin. *Scale bars*: 5 μm. *E,* IL-1α and IL-1β measured from culture supernatants of peritoneal macrophages from WT and *Ripk3*$^{-/-}$ upon exposure to the necrotic *Hmgb1*$^{-/-}$ or *Hmgb1*$^{+/+}$ MEF in the presence or absence of lipid IVa or lipid A (1 μg/ml). **, $p < 0.01$; ***, $p < 0.001$; ****, $p < 0.0001$. Graphs show the mean ± S.D. from three independent experiments.

release of IL-1α and IL-1β from WT but not *Tlr4*-deficient macrophages (Fig. 3*C*). Thus, HMGB1 and one of its receptors, TLR4, are critically involved in the Gram-negative bacterial lipid-induced RIPK3-dependent necroptosis, apoptosis, and IL-1 release.

TLRs rely on either MyD88 or TRIF for downstream signal transduction. Although for TLR3/TLR4, TRIF is a main driver of necroptosis by directly receptor-interacting protein (RIP) homotypic interaction motifs (RHIM) domain-dependent association with RIPK3, particularly when caspase-8 is absent or inhibited (25, 36–38). In this study, the genetic deletion of *Trif* abolished the HMGB1-lipid A/IVa complex induced release of LDH, IL-1α, and IL-1β (Fig. 3*D*), as well as the secretion of TNFα (Fig. 3*D*). As shown by flow cytometry, the deletion of *Trif* abrogated the HMGB1/lipid IVa or HMGB1/lipid

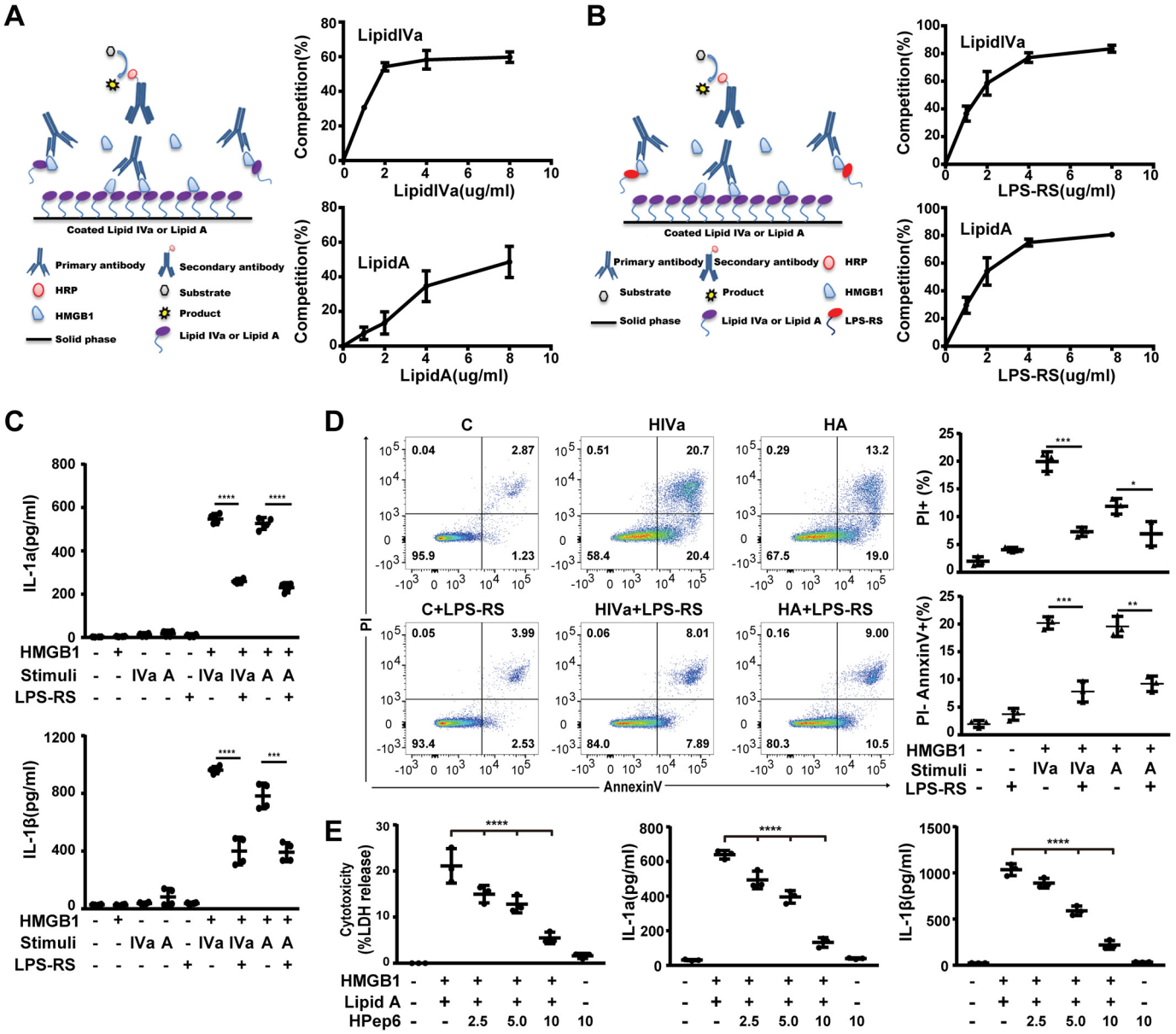

Figure 2. HMGB1 binding is critical for microbial lipids to trigger proinflammatory cell death. *A,* schematic illustration of competitive binding of HMGB1 by free lipid IVa or lipid A (*left*). Plates coated with lipid IVa or lipid A were incubated with recombinant HMGB1 (16 μg/ml) and the indicated concentrations of free lipid IVa or lipid A. After three extensive washings, the binding capacity between plate-coated lipid IVa or lipid A and HMGB1 was measured by using a HMGB1-specific primary antibody and relevant secondary antibodies. Then the percentage of binding competition by free lipid IVa or lipid A was evaluated. *B,* schematic illustration of competitive binding of HMGB1 by free LPS-RS (*left*). Plates coated with lipid IVa or lipid A (2 μg/ml) were incubated with HMGB1 (16 μg/ml) and the indicated concentration of LPS-RS. Then the percentage of binding competition by LPS-RS was evaluated. *C,* IL-1α and IL-1β were measured from the supernatants of mouse peritoneal macrophages stimulated with the indicated stimuli in the absence or presence of LPS-RS (2.5 μg/ml). *D,* the percentage of mouse peritoneal macrophages undergoing necrosis (PI^+) or apoptosis (PI^-) were measured by flow cytometry after stimulation with the indicated stimuli in the absence or presence of LPS-RS (2.5 μg/ml). *E,* LDH, IL-1α, and IL-1β in the supernatants of WT mouse peritoneal macrophages stimulated with lipid A (1 μg/ml) + HMGB1 (400 ng/ml) in the presence of different concentrations of HPep6 for 16 h. *, $p < 0.05$; **, $p < 0.01$; ***, $p < 0.001$; ****, $p < 0.0001$. Graphs show the mean ± S.D. from three independent experiments.

A-induced necroptosis and apoptosis in mouse peritoneal macrophages (Fig. 3*E*). Furthermore, necrotic lysate of WT MEFs facilitated the lipid IVa- or lipid A-induced release of IL-1α and IL-1β from WT, but not *Trif*-deficient macrophages (Fig. 3*F*). Using MyD88-deficient mice, we found that HMGB1 also significantly enhanced lipid A/IVa-induced production of TNFα and IL-6 in a MyD88-dependent manner (data not show).

Recent studies have suggested that the TLR4-TRIF signaling licenses Gram-negative bacteria to trigger caspase-11–dependent pyroptosis, a lytic form of programmed cell death, through type 1 interferon signaling (39, 40). Similarly, TLR4-TRIF signaling has also been suggested to promote bacteria-induced and the dsRNA-dependent kinase R (PKR)-dependent macrophage cell death. However, the deletion of *Caspase-11*, *Pkr*, or *Ifn-1R1*, the receptor of type 1 interferon, all failed to inhibit HMGB1/lipid IVa or HMGB1/lipid A-induced release of LDH, IL-1α, and IL-1β (Fig. 3*G*). Taken together, these findings have suggested the possible role of TLR4-TRIF-RIPK3 signaling in the regulation of HMGB1/lipid IVa or HMGB1/lipid A-induced necroptosis, apoptosis, and IL-1 release.

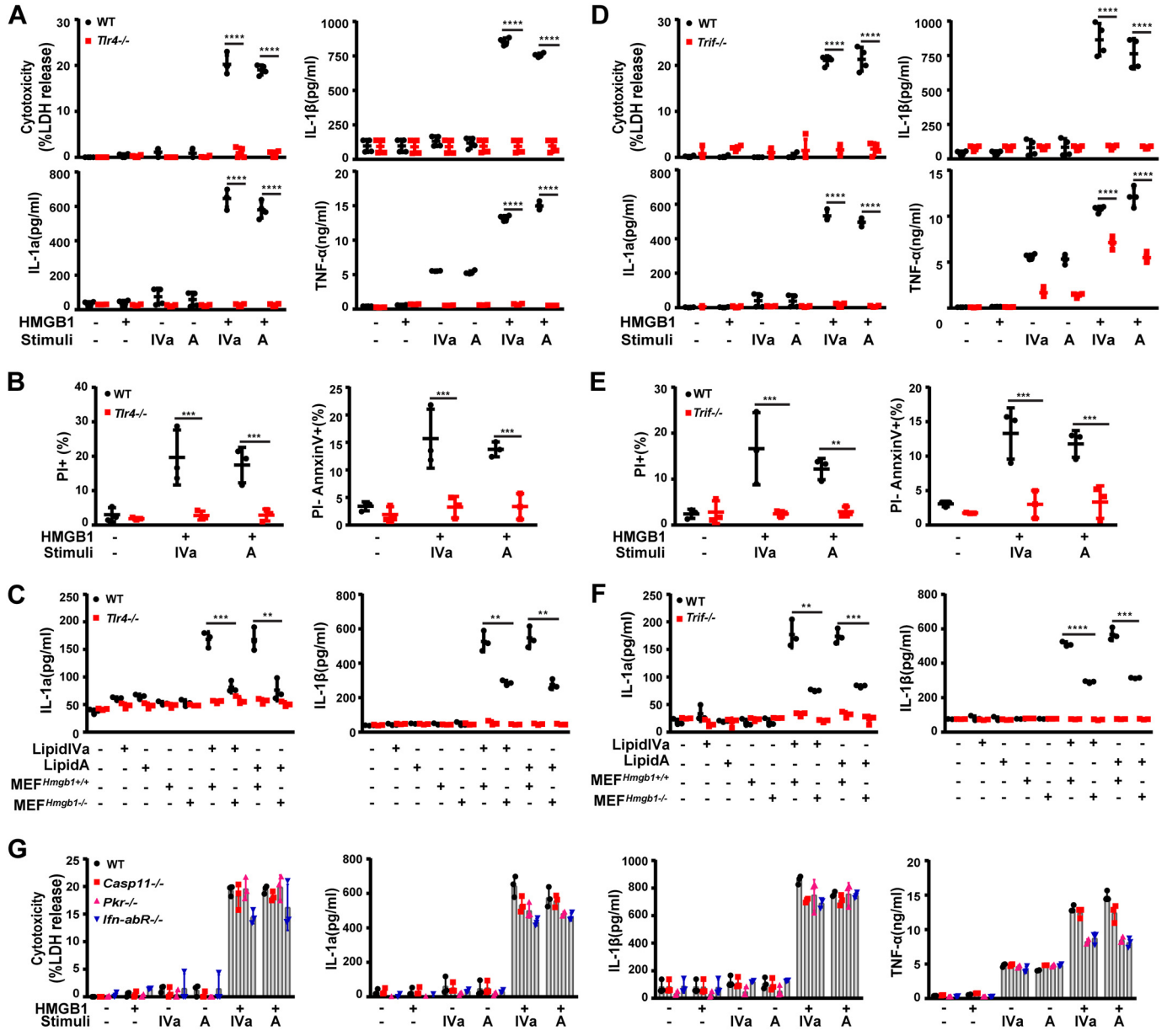

Figure 3. TLR4-TRIF signaling mediates HMGB1/microbial lipid-induced proinflammatory cell death. *A* and *D*, LDH, IL-1α, IL-1β, and TNFα were measured from culture supernatants of peritoneal macrophages from WT and *Tlr4*$^{-/-}$ or *Trif*$^{Lps/Lps2}$ mice stimulated with lipid IVa or lipid A (1 μg/ml) in the absence or presence of HMGB1 (0.4 μg/ml). *B* and *E*, flow cytometry analysis of the percentage of WT and *Tlr4*$^{-/-}$ or *Trif*$^{Lps/Lps2}$ macrophages undergoing necrosis (PI^+) or apoptosis (PI^-) after stimulation with lipid IVa or lipid A (1 μg/ml) in the presence of HMGB1 (0.4 μg/ml). *C* and *F*, IL-1α and IL-1β measured from the supernatants of peritoneal macrophages from WT and *Tlr4*$^{-/-}$ or *Trif*$^{Lps/Lps2}$ mice upon exposure to necrotic *Hmgb1*$^{-/-}$ or *Hmgb1*$^{+/+}$ MEF in the presence or absence of lipid IVa or lipid A (1 μg/ml). *G*, LDH, IL-1α, IL-1β, and TNFα measured from culture supernatants of peritoneal macrophages from mice with the indicated genotypes after stimulation with lipid IVa or lipid A (1 μg/ml) in the absence or presence of HMGB1 (0.4 μg/ml). *, $p < 0.05$; **, $p < 0.01$; ***, $p < 0.001$; ****, $p < 0.0001$. Graphs show the mean ± S.D. from three independent experiments.

MLKL mediates necroptosis induced by HMGB1 and bacterial lipids

RIPK3 mediates necroptosis through phosphorylation of its downstream substrate MLKL (41). Phosphorylated MLKL forms oligomers that disrupt the integrity of cell membranes, leading to necrotic cell death (41, 42). We thus determined whether co-addition of HMGB1 and bacterial lipids induces MLKL phosphorylation in RIPK3-deficient macrophages. Indeed, HMGB1/lipid IVa or HMGB1/lipid A induced MLKL phosphorylation in WT peritoneal macrophages (Fig. 4*A*). Similarly, the HMGB1/lipid IVa-induced MLKL phosphorylation was also attenuated by a specific RIPK3 kinase inhibitor (Fig. 4*A*). Similar observations were obtained from HMGB1/lipid A-stimulated cells (Fig. 4*B*). Moreover, the deletion of *Tlr4* or *Trif* markedly blocked HMGB1/lipid IVa or HMGB1/lipid A-induced MLKL phosphorylation (Fig. 4, *C–F*). Mechanistically, co-stimulation of macrophages with HMGB1 and lipid IVa or lipid A markedly enhanced the physical interaction between RIPK3 and MLKL (Fig. 4*G*). Given the essential role of MLKL in necroptosis, we next determined whether TLR4-TRIF signaling is required for the MLKL-driven necroptosis in macrophages. The deletion of *Mlkl* selectively blocked the

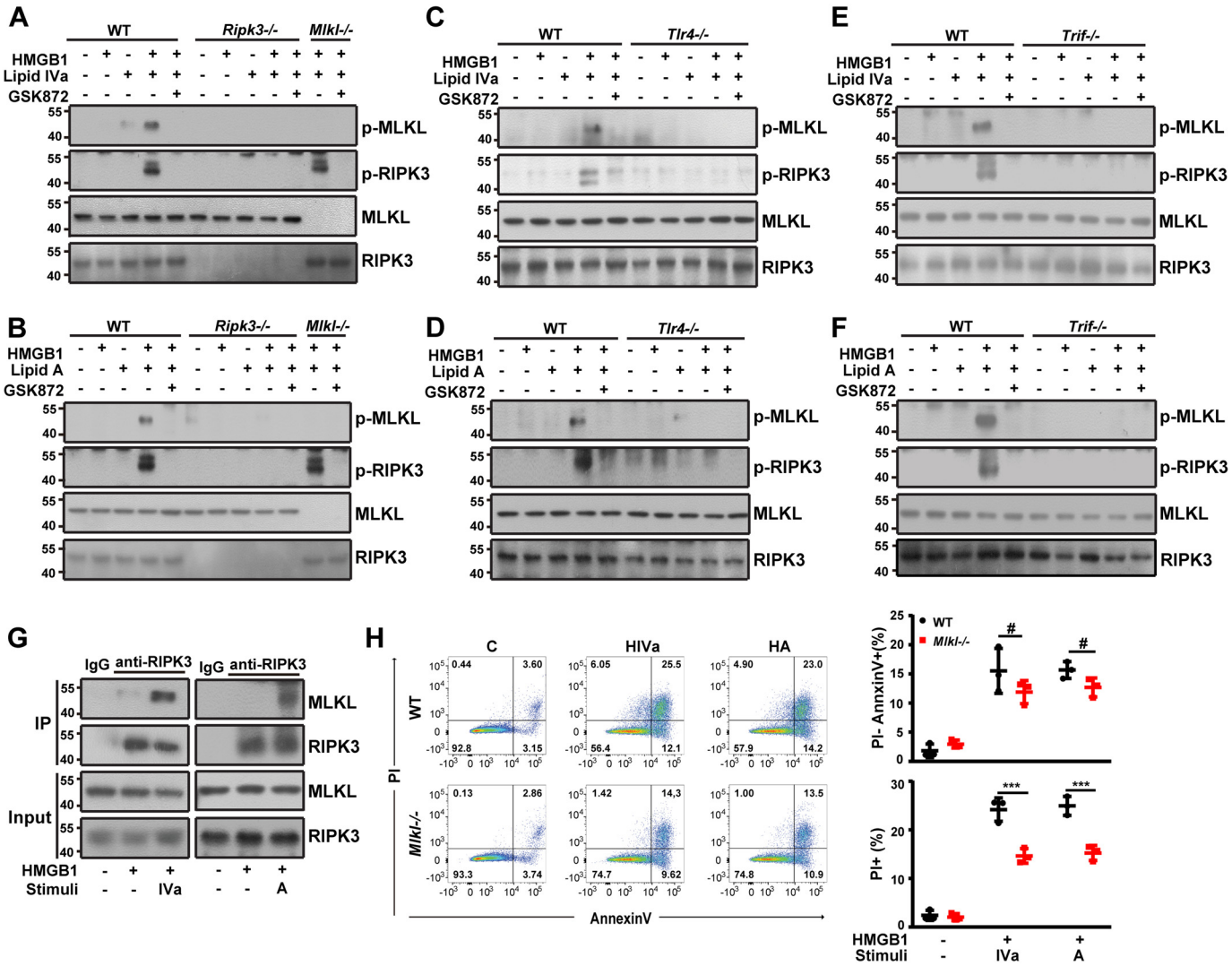

Figure 4. TLR4-TRIF-RIPK3 signaling mediates MLKL-dependent necroptosis induced by HMGB1 and microbial lipids. *A* and *B,* Western blot analysis of phosphorylated MLKL and RIPK3 in peritoneal macrophages from WT, *Ripk3*$^{-/-}$, and *Mlkl*$^{-/-}$ mice exposed to the indicated stimuli in the absence or presence of GSK872. *C* and *D,* Western blot analysis of phosphorylated MLKL and RIPK3 in peritoneal macrophages from WT and *Tlr4*$^{-/-}$ mice exposed to the indicated stimuli in the absence or presence of GSK872. *E* and *F,* Western blot analysis of phosphorylated MLKL and RIPK3 in peritoneal macrophages from WT and *Trif*$^{Lps/Lps2}$ mice exposed to the indicated stimuli in the absence or presence of GSK872. *G,* cell lysates of peritoneal macrophages from a WT mouse treated with the indicated stimuli were immunoprecipitated (*IP*) with RIPK3-specific antibody. The precipitated proteins were immunoblotted with RIPK3- or MLKL-specific antibodies. Whole cell lysate (*Input*) was used as positive control. *H,* flow cytometry analysis of the percentage of WT or *Mlkl*$^{-/-}$ peritoneal macrophages undergoing necrosis (PI^+) or apoptosis (PI^-) following stimulation with lipid IVa or lipid A (1 μg/ml) in the presence of HMGB1 (0.4 μg/ml). ***, $p < 0.001$; #, not significant. Graphs show the mean ± S.D. from three independent experiments.

HMGB1/lipid IVa- or HMGB1/lipid A-induced necroptosis (Fig. 4*H*); whereas the deletion of *Tlr4*, *Trif*, or *Ripk3* blocked both necroptosis and apoptosis in mouse peritoneal macrophages (Figs. 1 and 3). Together, these findings indicate that TLR4-TRIF-RIPK3 signaling activates parallel MLKL-dependent necroptosis and MLKL-independent apoptosis in response to stimulation with HMGB1 and bacterial lipids.

Caspase-8 mediates apoptosis induced by HMGB1 and bacterial lipids

In response to IAV infection, RIPK3 also mediates caspase-8–dependent apoptosis in a mechanism independent of its kinase activity (43). To test whether HMGB1/lipid IVa or HMGB1/lipid A could activate caspase-8 in a RIPK3-dependent fashion, we measured the levels of caspase-8 cleavage as an indicator of its activation. The co-addition of HMGB1 enhanced the lipid IVa- or lipid A-induced caspase-8 cleavage (Fig. 5*A*), which was barely inducible if HMGB1, lipid IVa, or lipid A was added alone (Fig. 5*A*). The deletion of RIPK3, but not MLKL, blocked the HMGB1/lipid IVa- or HMGB1/lipid A-induced caspase-8 cleavage (Fig. 5, *A–C*). Likewise, pharmacological inhibition of caspase-8 similarly abrogated the HMGB1/lipid IVa- or HMGB1/lipid A-induced caspase-8 cleavage in both WT and *Mlkl*-deficient macrophages (Fig. 5, *B* and *C*). Moreover, the deletion of *Tlr4* or *Trif* also blocked the HMGB1/lipid IVa or HMGB1/lipid A-induced caspase-8 cleavage (Fig. 5, *E–H*). Together with the finding that the deletion of *Tlr4*, *Trif*, or *Ripk3* blocked HMGB1/lipid-induced apoptosis, these results indicate that TLR4-TRIF-RIPK3 signaling occupies an important role in the HMGB1/bacterial

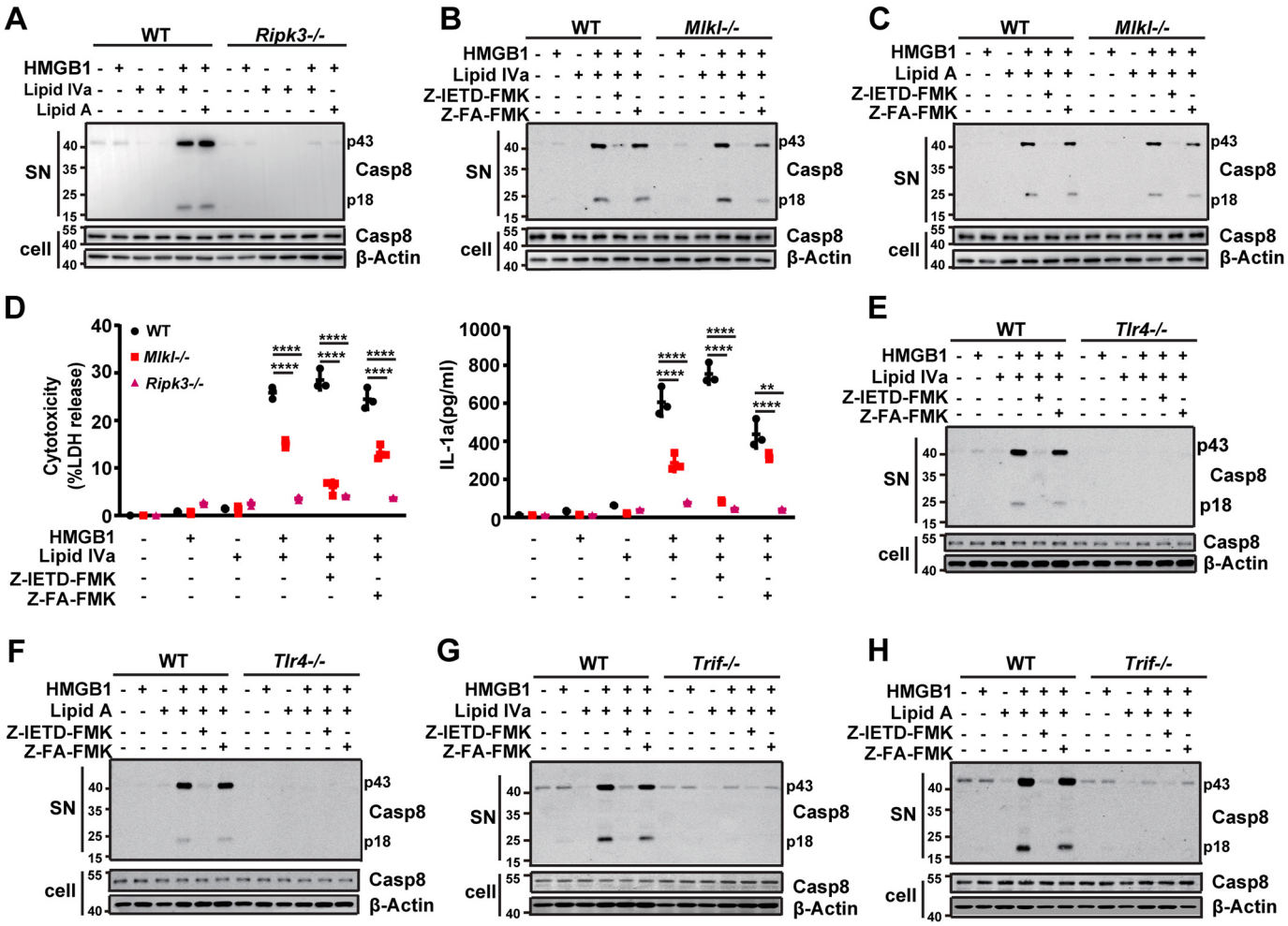

Figure 5. TLR4-TRIF-RIPK3 signaling mediates caspase-8–dependent apoptosis induced by HMGB1 and microbial lipids. *A,* Western blot analysis of processed caspase-8 released from WT and *Ripk3*$^{-/-}$ mouse peritoneal macrophages stimulated with lipid IVa or lipid A (1 μg/ml) in the absence or presence of HMGB1 (0.4 μg/ml). *B* and *C,* Western blot assay for processed caspase-8 released from WT and *Mlkl*$^{-/-}$ mouse peritoneal macrophages exposed to the indicated stimuli in the absence or presence of caspase-8 inhibitor or control. *D,* LDH and IL-1α measured from culture supernatants of peritoneal macrophages from WT, *Ripk3*$^{-/-}$, and *Mlkl*$^{-/-}$ mice exposed to the indicated stimuli in the absence or presence of caspase-8 inhibitor or controls. *E* and *F,* Western blot assay for processed caspase-8 released from WT and *Tlr4*$^{-/-}$ mouse peritoneal macrophages exposed to the indicated stimuli in the absence or presence of caspase-8 inhibitor or control. *G* and *H,* Western blot for processed caspase-8 released from WT and *Trif*$^{Lps/Lps2}$ mouse peritoneal macrophages exposed to the indicated stimuli in the absence or presence of caspase-8 inhibitor or control. **, $p < 0.01$; ****, $p < 0.0001$. Graphs show the mean ± S.D. from three independent experiments.

lipid-mediated and caspase-8–dependent apoptosis in innate immune cells.

Although *Ripk3* deficiency almost led to a complete blockade of HMGB1/lipid IVa- or HMGB1/lipid A-induced release of LDH and IL-1α, the deletion of *Mlkl* only partially inhibited the HMGB1/lipid-induced release of LDH and IL-1α (Fig. 5*D*). Notably, addition of the caspase-8 inhibitor significantly inhibited the HMGB1/lipid-induced LDH and IL-1α release in *Mlkl*-deficient, but not in WT, macrophages (Fig. 5*D*). Thus, it appears that HMGB1 enables lipid IVa or lipid A to activate parallel MLKL-dependent necroptosis and caspase-8–dependent apoptosis through TLR4-TRIF-RIPK3 signaling, ultimately leading to IL-1α release.

RIPK3 mediates NLRP3 inflammasome-dependent IL-1β cleavage and release in response to HMGB1 and bacterial lipids

During IAV infection, RIPK3 is required for activation of the NLRP3 inflammasome, which are intracellular protein complexes that mediate IL-1β maturation and release through caspase-1 (30). To test whether TLR4-TRIF-RIPK3 signaling is essential for the NLRP3 inflammasome-dependent IL-1β maturation and release, peritoneal macrophages from WT, *Ripk3*-deficient, *Nlrp3*-deficient, and *Asc*-deficient mice were stimulated with lipid IVa or lipid A in the absence or presence of HMGB1. The deletion of *Ripk3*, *Nlrp3*, or *Asc* blocked the HMGB1/lipid IVa- or HMGB1/lipid A-induced IL-1β release and maturation, whereas deletion of *Ripk3*, *Nlrp3,* or *Asc* did not alter the expression of the cytokines tested (Fig. 6, *A–C*, Fig. S4). Furthermore, inhibition of necroptosis by necrostatin-1 significantly reduced the release of IL-1α and IL-1β induced by HMGB1 + lipid IVa/A (Fig. S5). Likewise, the deletion of *Tlr4*, *Trif*, or *Ripk3* similarly abrogated the HMGB1/lipid IVa- or HMGB1/lipid A-induced release of both IL-1α and IL-1β (Figs. 1, 3, and 6*D*), which was in sharp contrast to the findings obtained from using the *Nlrp3*- or *Asc*-deficient macrophages (Fig. 6, *A* and *B*). Together, these data demonstrate that TLR4-TRIF-RIPK3 signaling mediates both NLRP3 inflam-

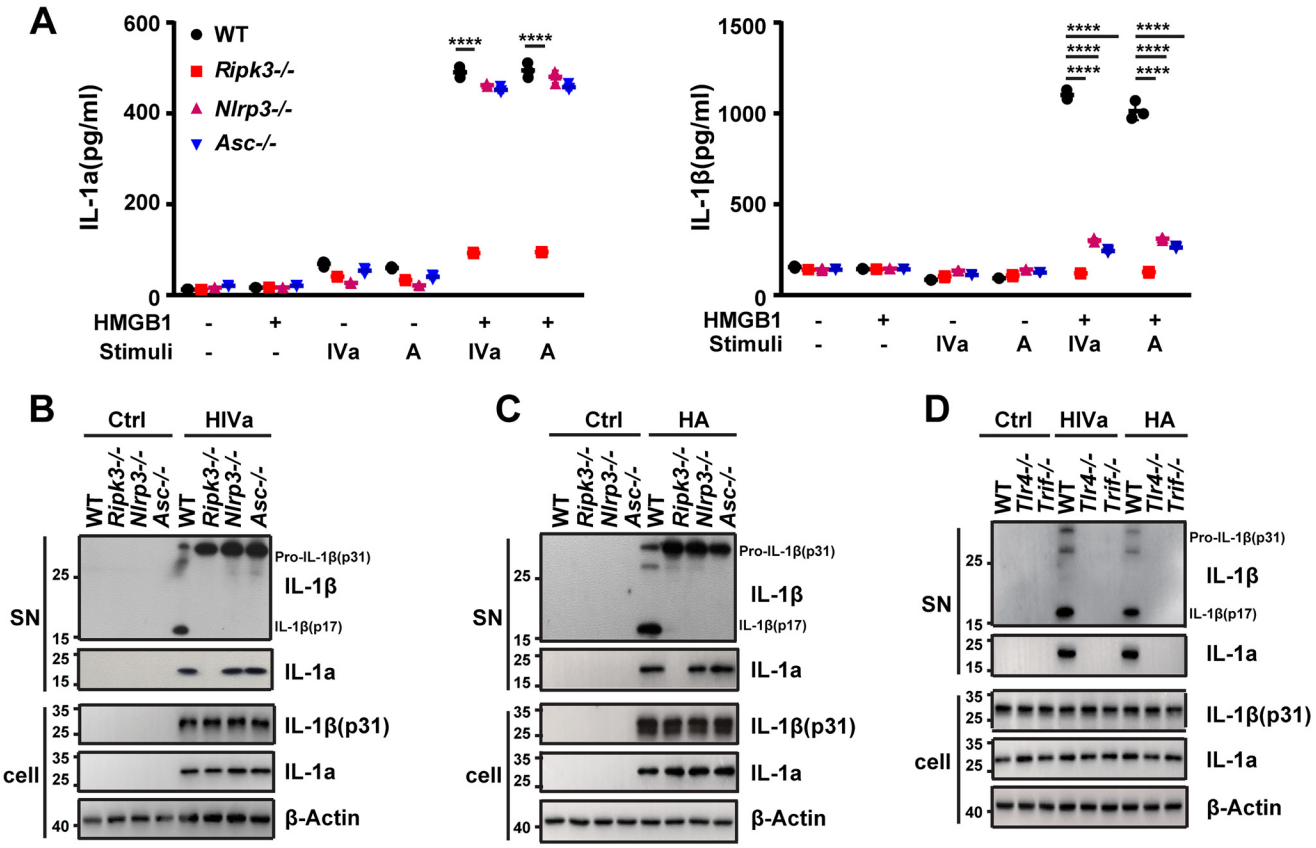

Figure 6. RIPK3 mediates the NLRP3 inflammasome-dependent IL-1β cleavage and release in response to HMGB1 and microbial lipids. *A,* IL-1α and IL-1β measured from culture supernatants of peritoneal macrophages from WT, *Ripk3*$^{-/-}$, *Nlrp3*$^{-/-}$, and *Asc*$^{-/-}$ mice stimulated with lipid IVa or lipid A (1 μg/ml) in the absence or presence of HMGB1 (0.4 μg/ml). *B* and *C,* Western blot analysis of IL-1α and IL-1β released from mouse peritoneal macrophages with the indicated genotypes stimulated with lipid IVa (1 μg/ml) + HMGB1 (0.4 μg/ml) (*B*) or lipid A (1 μg/ml) + HMGB1 (0.4 μg/ml) (*C*). *D,* Western blot analysis of processed IL-1α and IL-1β released from mouse peritoneal macrophages with the indicated genotypes stimulated with lipid IVa (1 μg/ml) + HMGB1 (0.4 μg/ml) or lipid A (1 μg/ml) + HMGB1 (0.4 μg/ml). *, $p < 0.05$; **, $p < 0.01$; ***, $p < 0.001$; ****, $p < 0.0001$; #, not significant. Graphs show the mean ± S.D. from three independent experiments.

masome-dependent IL-1β maturation and inflammasome-independent IL-1α release in response to HMGB1 and bacterial lipids.

The role of RIPK3 and HMGB1 in bacteria-induced nonresolving inflammation

As IL-1R is the receptor of both IL-1α and IL-1β, we next investigated whether TRIF-RIPK3-IL-1R signaling regulates inflammatory responses induced by Gram-negative bacteria, which releases their components (including lipid IVa and lipid A) to stimulate robust HMGB1 secretion from immune cells. In an air-pouch inflammatory infiltration model, injection of live *Escherichia coli* resulted in a persistent infiltration of leukocytes, including neutrophils and macrophages, which were completely blocked by the genetic deletion of *Ripk3* (Fig. 7*A*). To determine whether the diminished leukocyte infiltration is because of increased bacterial clearance or enhanced inflammation resolution, heat-killed *E. coli* was injected into the air pouch. The genetic *Ripk3* knockout prevented the *E. coli*-induced persistent infiltration of neutrophils and macrophages even at 5 days after infection (Fig. 7*B*). The deletion of *Trif* or *Il-1R* phenocopied the observed *Ripk3* deficiency in this model (Fig. 7*C*). Furthermore, neutralizing extracellular HMGB1 by monoclonal antibodies abrogated the Gram-negative bacteria-induced infiltration of total leukocytes, neutrophils, and macrophages (Fig. 7*E*). Anti-HMGB1 antibody treatment also significantly inhibited necroptosis and apoptosis of infiltrated cells and proinflammatory cytokines' production (Fig. S6). Together, these findings indicate that extracellular HMGB1 promotes bacteria-induced nonresolving inflammation through the TRIF-RIPK3-IL-1R signaling.

Discussion

Previous studies show that RIPK3 deficiency prevents axonal degeneration in ALS, improves survival following kidney/heart ischemia-reperfusion injury or ethanol/acetaminophen-induced liver injury, and renders animals more susceptible to several types of DNA or RNA virus, such as vaccinia virus, IAV, and West Nile virus (23, 28, 30, 43–47). However, the roles of RIPK3 in bacterial infection and the mechanisms by which bacterial components activate RIPK3 in innate immune cells remain largely unknown. In the current study, our data establishes that HMGB1 enables lipid IVa or lipid A to activate parallel MLKL-dependent necroptosis and caspase-8–dependent apoptosis through TLR4-TRIF-RIPK3 signaling. Lipid IVa and lipid A are abundant microbial lipids in Gram-negative bacteria. Considering that HMGB1 and RIPK3 are highly evolutionarily conserved in mammals (2, 3), it is conceivable that

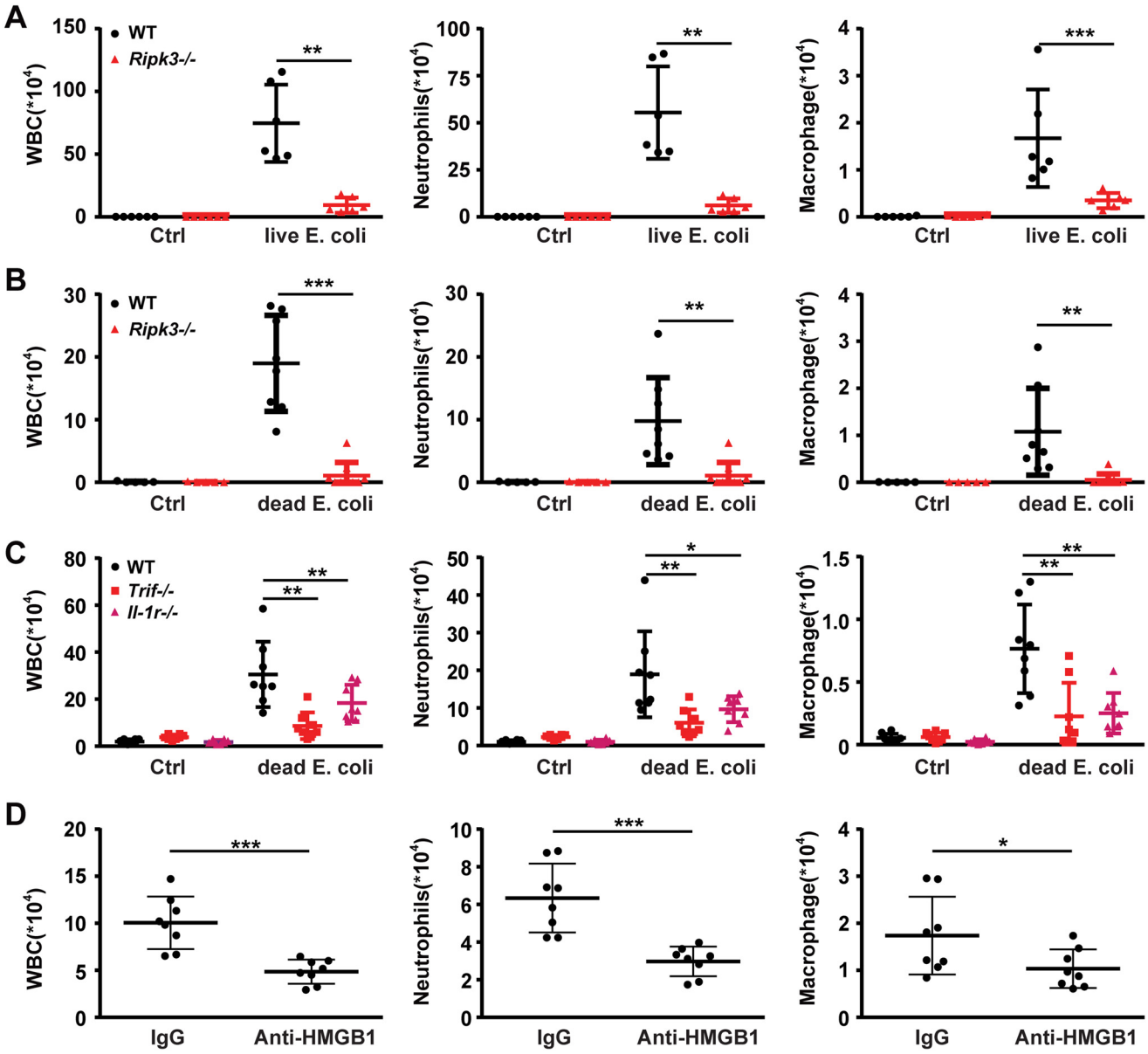

Figure 7. Loss of RIPK3 attenuates inflammation induced by dead *E. coli* and HMGB1. *A,* air-pouch lavage fluid was collected from WT and *Ripk3*$^{-/-}$ mice following injection with live *E. coli* for analysis of infiltrated white blood cell (*WBC*) counts by microscope (*left*) and neutrophils (*middle*) and macrophages (*right*) by flow cytometry. *B,* air-pouch lavage fluid was collected from WT and *Ripk3*$^{-/-}$ mice following injection with heat-killed *E. coli* for analysis of infiltrated white blood cell counts by microscope (*left*) and neutrophils (*middle*) and macrophages (*right*) by flow cytometry. *C,* WT, *Trif*$^{Lps/Lps2}$ mice and *Il-1R*$^{-/-}$ mice were selected for the same experiment as *B,* and leukocytes (*left*), neutrophils (*middle*), and macrophages (*right*) numbers are shown. *D,* air-pouch inflammatory infiltration was induced in the absence or presence of HMGB1-neutralizing or normal control IgGs. Then air-pouch lavage fluid was collected, and leukocytes (*left*), neutrophils (*middle*), and macrophages (*right*) numbers are shown. *Circles* represent individual mice. *, $p < 0.05$; **, $p < 0.01$; ***, $p < 0.001$. Graphs show the mean ± S.D. from three independent experiments.

HMGB1 and microbial lipid-induced RIPK3 signaling might confer protection against certain pathogens in natural history. Lipid IVa has been reported as an antagonist in human, but not mouse (48). In agreement with these findings, we observed that the HMGB1-lipid IVa complex could trigger cell death and inflammatory responses in mouse macrophages, but not human PBMCs. A recent study reports that the TLR4-TRIF-RIPK3 signaling can be activated by *Yersinia pestis*, a Gram-negative bacterium infamous for its large pandemics such as the "Black Death" in medieval Europe (49). Mice defective in RIPK3 are highly susceptible to *Y. pestis* infection (49). However, these protective immune responses against pathogens, such as *Y. pestis,* might come at the cost of causing none-resolving inflammation.

In this study, we found that RIPK3 mediates a nonresolving inflammation during *E. coli* infection through IL-1R signaling, which is critical for leukocyte infiltration. It is known that cells undergoing MLKL-dependent necroptosis could passively release abundant IL-1α into the extracellular space (29). However, the deletion of *Mlkl* only partially inhibits IL-1α release in HMGB1 and bacterial lipid-stimulated macrophages. Additionally, the inhibition of caspase-8 almost completely blocks the IL-1α release in *Mlkl*-deficient macrophages. These findings are surprising because it was previously believed that apo-

ptotic cells do not release DAMPs. Recent advances reveal that caspase-3 not only mediates apoptosis but also is able to induce programmed necrosis by cleaving its substrate gasdermin E (GSDME) (50). Upon activation by caspase-3, GSDME binds to the cell membranes and functions as pore-forming peptides that execute necrotic cell death (50). Thus, these findings raise an intriguing possibility that activated caspase-3 might induce IL-1α release by cleaving GSDME in HMGB1/bacterial lipid-stimulated macrophages.

One remaining question is what dictates whether RIPK3 triggers necroptosis or apoptosis in response to HMGB1/bacterial lipids? This stochastic decision may be determined by local availability of MLKL *versus* caspase-8 in the cells. For example, HMGB1/bacterial lipids might trigger necroptosis in cells that fail to sufficiently activate caspase-8 to over-balance or suppress the RIPK3-dependent MLKL phosphorylation. The fact that HMGB1 + bacterial lipids induces necroptosis without concurrent caspase-8 suppression lends support to the "stochastic availability" model, in which both apoptosis and necroptosis can be equivalently deployed downstream of RIPK3. Another observation in our study that supports the stochastic availability model is that pharmacological inhibition of caspase-8 significantly promotes HMGB1/bacterial lipid-induced necroptosis (data not shown). In conclusion, our study identifies a novel role of RIPK3 in bacteria-induced nonresolving inflammation, and uncovers a previously unrecognized mechanism by which HMGB1 and bacterial components work in concert to orchestrate RIPK3-dependent immune responses under physiological conditions.

Experimental procedures

Mice

The *Trif*$^{Lps/Lps2}$, *Caspase-11*$^{-/-}$, and *Il1-R*$^{-/-}$ mice were purchased from the Jackson Laboratory. The *Ripk3*$^{-/-}$ and *Mlkl*$^{-/-}$ mice were generous gifts from Dr. Jiahuai Han. The *Pkr*$^{-/-}$ mice were generous gifts from Dr. Kevin J. Tracey. The *Nlrp3*$^{-/-}$ and *Asc*$^{-/-}$ mice were generous gifts from Dr. Rongbin Zhou. The *Tlr4*$^{-/-}$ mice were generous gifts from Dr. Shusheng Gong. The *Ifn*$\alpha\beta R^{-/-}$ mice were a generous gift from Dr. Jin Hou. Experimental groups were sex matched and 8–12 weeks of age. Animals were held under specific pathogen-free conditions and maintained in the Central South University Animal Facility with water and standard diet. All animal experiments were approved and performed according to the Guidelines for Animal Experiments by the Institutional Animal Care and Use Committees of Central South University.

Reagents

Lipid IVa(24006-S) was purchased from the Peptide Institute. Lipid A (L5399) was purchased from Sigma. Highly purified recombinant HMGB1 protein was provided by Dr. Kevin J. Tracey. Z-IETD-fmk (550380) and Z-FA-fmk (550411) were purchased from BD Bioscience. GSK872 was obtained from Merck. Antibodies IL-1α (ab9724), phosphorylated MLKL (Ser-345) (ab196436), phosphorylated RIPK3 (Ser-232) (ab195117), and HMGB1 (clone EPR3507) were from Abcam. Antibodies against Caspase-8(4927S), cleaved Caspase-8 (Asp-387)(8592S), MLKL(28640S), and RIPK1 (3493S) were purchased from Cell Signaling Technologies. Antibody against RIPK3 (17563-1-AP) was purchased from Proteinteck. Antibody against IL-1β (AF-401-NA) was purchased from R&D Systems Inc.

Macrophage preparation and stimulation

Mouse peritoneal macrophages were isolated and cultured as described previously (4). Briefly, mice (8–12 weeks old) were injected intraperitoneally with thioglycollate broth to elicit peritoneal macrophages. Cells were collected and resuspended in RPMI 1640 medium (Gibco) supplemented with 10% fetal calf serum and antibiotics (Gibco). Peritoneal macrophages were stimulated with lipid IVa/lipid A and HMGB1 as indicated. In some experiments, cells were pretreated with 15 μM Z-IETD-fmk or 15 μM Z-FA-fmk for 0.5 h before infection. Cell lysates and supernatants were collected 16 h later for Western blotting, ELISA, and LDH release.

Cell death assays

Cell death was assessed by LDH Cytotoxicity Assay kit (Beyotime Biotechnology) according to the manufacturer's instructions.

Western blot

Protein samples were separated by 15% SDS-PAGE and transferred onto polyvinylidene difluoride membranes (Millipore). Membranes were then incubated with antibodies as indicated. Blots were normalized to β-actin expression (1:5000 dilutions, Cell Signaling Technology).

Creation of air-pouch in mice

Creation of the air-pouch was performed as described previously (51). The mice were shaved in their dorsal region, and then 0.2 μm of filtered air (5 and 3 ml) was subcutaneously injected (on days 0 and 3, respectively). The mice were anesthetized with isoflurane at day 0 to ensure compliance and reduce pain. On day 6, inflammation was induced by intrapouch injection of PBS or bacteria solution (live/heat-killed *E. coli*, 5×10^6). Five days after infection, cells in the air-pouch were collected. Cell counting was performed by a hemacytometer. For analyses of specific populations in the air-pouch, cells were stained with antibodies against CD45, F4/80, Ly-6G, and CD11b (eBioscience) and analyzed on the FACS Canto (BD Bioscience) instrument.

Competitive ELISA

Corning Costar ELISA were coated with 2 μg/ml of lipid IVa or lipid A, and blocked with 0.25% casein for 2 h at room temperature. HMGB1 (16 μg/ml) and lipid IVa/lipid A (1$\sim$8 μg/ml) or RS-LPS (1$\sim$8 μg/ml) was added to the wells and incubated for 0.5 h at 37 °C. HMGB1 antibody (1:5000) (ab79823) was incubated for an additional 0.5 h at 37 °C. Goat anti-rabbit IgG H&L (horseradish peroxidase) was incubated for an additional 1.5 h. Tetramethylbenzidine solution was used for color.

Apoptosis and cell death assay

The peritoneal macrophage (about 1×10^6 cells) were treated with either vehicle or stimulis for 16 h, as indicated,

washed with PBS and trypsinized before re-suspending them in the appropriate media. Cells were then stained with FITC-labeled annexin V and propidium iodide (PI) and detected by fluorescence-activated cell sorter (FACS) analysis. Storing and processing of data were done with FlowJo software.

Transmission EM

Transmission EM was performed as described previously (52). In brief, cells treated with HMGB1 alone or HMGB1/lipid IVa or HMGB1/lipid A were harvested and fixed with 2.5% glutaraldehyde in PBS (pH 7.2) for 4 h. Ultra-thin sections were cut and observed under an H-600IV transmission electron microscope (Hitachi, Tokyo, Japan).

Isolation and in vitro activation of PBMCs

Human blood from adult healthy volunteers' collection was approved by the research ethics committee of The 3rd Xiangya Hospital of Central South University. Experiments with human PBMCs were abided by the Helsinki Declaration for experiments involving humans. PBMCs were isolated using Ficoll-Paque density gradient media (GE Healthcare). After centrifugation, PBMCs were resuspended in RPMI 1640 medium supplemented with 10% fetal bovine serum and antibiotics and stimulated with lipid IVa/lipid A and HMGB1 as indicated for 16 h. Cell supernatants were collected for ELISA.

Statistical analysis

All data were analyzed using GraphPad Prism software (version 5.01). Data were analyzed by Student's t test for comparison between two groups or one-way analysis of variance followed by a post hoc Bonferroni test for multiple comparisons. A p value <0.05 was considered statistically significant for all experiments. All values are presented as the mean ± S.D.

Author contributions—R. M. and L. G. data curation; R. M. formal analysis; R. M., L. G., Y. L., K. Z., J. W., J. H., and Y. T. methodology; R. M. writing-original draft; Y. L. software; Y. L. and B. L. project administration; K. Z. and Y. T. supervision; K. Z. and H. W. writing-review and editing; J. W., H. W., and J. H. resources; J. H. and B. L. conceptualization; Y. T. and B. L. funding acquisition.

Acknowledgment—We thank Dr. Kevin J. Tracey for the kind gifts of highly purified recombinant HMGB1 protein and neutralizing anti-HMGB1 mAb.

References

1. Takeuchi, O., and Akira, S. (2010) Pattern recognition receptors and inflammation. *Cell* **140,** 805–820 CrossRef Medline
2. Tang, Y., Zhao, X., Antoine, D., Xiao, X., Wang, H., Andersson, U., Billiar, T. R., Tracey, K. J., and Lu, B. (2016) Regulation of posttranslational modifications of HMGB1 during immune responses. *Antioxid. Redox Signal.* **24,** 620–634 Medline
3. Lu, B., Wang, C., Wang, M., Li, W., Chen, F., Tracey, K. J., and Wang, H. (2014) Molecular mechanism and therapeutic modulation of high mobility group box 1 release and action: an updated review. *Expert Rev. Clin. Immunol.* **10,** 713–727 CrossRef Medline
4. Lu, B., Nakamura, T., Inouye, K., Li, J., Tang, Y., Lundbäck, P., Valdes-Ferrer, S. I., Olofsson, P. S., Kalb, T., Roth, J., Zou, Y., Erlandsson-Harris, H., Yang, H., Ting, J. P., Wang, H. *et al.* (2012) Novel role of PKR in inflammasome activation and HMGB1 release. *Nature* **488,** 670–674 CrossRef Medline
5. Lu, B., Antoine, D. J., Kwan, K., Lundbäck, P., Wähämaa, H., Schierbeck, H., Robinson, M., Van Zoelen, M. A., Yang, H., Li, J., Erlandsson-Harris, H., Chavan, S. S., Wang, H., *et al.* (2014) JAK/STAT1 signaling promotes HMGB1 hyperacetylation and nuclear translocation. *Proc. Natl. Acad. Sci. U.S.A.* **111,** 3068–3073 CrossRef Medline
6. Wang, H., Bloom, O., Zhang, M., Vishnubhakat, J. M., Ombrellino, M., Che, J., Frazier, A., Yang, H., Ivanova, S., Borovikova, L., Manogue, K. R., Faist, E., Abraham, E., Andersson, J., Andersson, U., *et al.* (1999) HMG-1 as a late mediator of endotoxin lethality in mice. *Science* **285,** 248–251 CrossRef Medline
7. Scaffidi, P., Misteli, T., and Bianchi, M. E. (2002) Release of chromatin protein HMGB1 by necrotic cells triggers inflammation. *Nature* **418,** 191–195 CrossRef Medline
8. Wang, H., Liao, H., Ochani, M., Justiniani, M., Lin, X., Yang, L., Al-Abed, Y., Wang, H., Metz, C., Miller, E. J., Tracey, K. J., and Ulloa, L. (2004) Cholinergic agonists inhibit HMGB1 release and improve survival in experimental sepsis. *Nat. Med.* **10,** 1216–1221 CrossRef Medline
9. Tsung, A., Sahai, R., Tanaka, H., Nakao, A., Fink, M. P., Lotze, M. T., Yang, H., Li, J., Tracey, K. J., Geller, D. A., and Billiar, T. R. (2005) The nuclear factor HMGB1 mediates hepatic injury after murine liver ischemia-reperfusion. *J. Exp. Med.* **201,** 1135–1143 CrossRef Medline
10. Apetoh, L., Ghiringhelli, F., Tesniere, A., Obeid, M., Ortiz, C., Criollo, A., Mignot, G., Maiuri, M. C., Ullrich, E., Saulnier, P., Yang, H., Amigorena, S., Ryffel, B., Barrat, F. J., Saftig, P., *et al.* (2007) Toll-like receptor 4-dependent contribution of the immune system to anticancer chemotherapy and radiotherapy. *Nat. Med.* **13,** 1050–1059 CrossRef Medline
11. Tian, J., Avalos, A. M., Mao, S. Y., Chen, B., Senthil, K., Wu, H., Parroche, P., Drabic, S., Golenbock, D., Sirois, C., Hua, J., An, L. L., Audoly, L., La Rosa, G., Bierhaus, A., *et al.* (2007) Toll-like receptor 9-dependent activation by DNA-containing immune complexes is mediated by HMGB1 and RAGE. *Nat. Immunol.* **8,** 487–496 CrossRef Medline
12. Kazama, H., Ricci, J. E., Herndon, J. M., Hoppe, G., Green, D. R., and Ferguson, T. A. (2008) Induction of immunological tolerance by apoptotic cells requires caspase-dependent oxidation of high-mobility group box-1 protein. *Immunity* **29,** 21–32 CrossRef Medline
13. Rittirsch, D., Flierl, M. A., Nadeau, B. A., Day, D. E., Huber-Lang, M., Mackay, C. R., Zetoune, F. S., Gerard, N. P., Cianflone, K., Köhl, J., Gerard, C., Sarma, J. V., and Ward, P. A. (2008) Functional roles for C5a receptors in sepsis. *Nat. Med.* **14,** 551–557 CrossRef Medline
14. Yanai, H., Ban, T., Wang, Z., Choi, M. K., Kawamura, T., Negishi, H., Nakasato, M., Lu, Y., Hangai, S., Koshiba, R., Savitsky, D., Ronfani, L., Akira, S., Bianchi, M. E., Honda, K., *et al.* (2009) HMGB proteins function as universal sentinels for nucleic-acid-mediated innate immune responses. *Nature* **462,** 99–103 CrossRef Medline
15. Maroso, M., Balosso, S., Ravizza, T., Liu, J., Aronica, E., Iyer, A. M., Rossetti, C., Molteni, M., Casalgrandi, M., Manfredi, A. A., Bianchi, M. E., and Vezzani, A. (2010) Toll-like receptor 4 and high-mobility group box-1 are involved in ictogenesis and can be targeted to reduce seizures. *Nat. Med.* **16,** 413–419 CrossRef Medline
16. Bald, T., Quast, T., Landsberg, J., Rogava, M., Glodde, N., Lopez-Ramos, D., Kohlmeyer, J., Riesenberg, S., van den Boorn-Konijnenberg, D., Hömig-Hölzel, C., Reuten, R., Schadow, B., Weighardt, H., Wenzel, D., Helfrich, I., *et al.* (2014) Ultraviolet-radiation-induced inflammation promotes angiotropism and metastasis in melanoma. *Nature* **507,** 109–113 CrossRef Medline
17. Huebener, P., Pradere, J. P., Hernandez, C., Gwak, G. Y., Caviglia, J. M., Mu, X., Loike, J. D., Jenkins, R. E., Antoine, D. J., and Schwabe, R. F. (2015) The HMGB1/RAGE axis triggers neutrophil-mediated injury amplification following necrosis. *J. Clin. Investig.* **125,** 539–550 CrossRef Medline
18. Tirone, M., Tran, N. L., Ceriotti, C., Gorzanelli, A., Canepari, M., Bottinelli, R., Raucci, A., Di Maggio, S., Santiago, C., Mellado, M., Saclier, M., François, S., Careccia, G., He, M., De Marchis, F., *et al.* (2018) High mo-

bility group box 1 orchestrates tissue regeneration via CXCR4. *J. Exp. Med.* **215,** 303–318 CrossRef Medline

19. Youn, J. H., Oh, Y. J., Kim, E. S., Choi, J. E., and Shin, J. S. (2008) High mobility group box 1 protein binding to lipopolysaccharide facilitates transfer of lipopolysaccharide to CD14 and enhances lipopolysaccharide-mediated TNF-alpha production in human monocytes. *J. Immunol.* **180,** 5067–5074 CrossRef
20. Yang, J., Zhao, Y., Zhang, P., Li, Y., Yang, Y., Yang, Y., Zhu, J., Song, X., Jiang, G., and Fan, J. (2016) Hemorrhagic shock primes for lung vascular endothelial cell pyroptosis: role in pulmonary inflammation following LPS. *Cell Death Dis.* **7,** e2363 CrossRef Medline
21. Deng, M., Tang, Y., Li, W., Wang, X., Zhang, R., Zhang, X., Zhao, X., Liu, J., Tang, C., Liu, Z., Huang, Y., Peng, H., Xiao, L., Tang, D., Scott, M. J., *et al.* (2018) The endotoxin delivery protein HMGB1 mediates caspase-11-dependent lethality in sepsis. *Immunity* **49,** 740–753.e7 CrossRef Medline
22. He, S., Wang, L., Miao, L., Wang, T., Du, F., Zhao, L., and Wang, X. (2009) Receptor interacting protein kinase-3 determines cellular necrotic response to TNF-α. *Cell* **137,** 1100–1111 CrossRef Medline
23. Cho, Y. S., Challa, S., Moquin, D., Genga, R., Ray, T. D., Guildford, M., and Chan, F. K. (2009) Phosphorylation-driven assembly of the RIP1-RIP3 complex regulates programmed necrosis and virus-induced inflammation. *Cell* **137,** 1112–1123 CrossRef Medline
24. Zhang, D. W., Shao, J., Lin, J., Zhang, N., Lu, B. J., Lin, S. C., Dong, M. Q., and Han, J. (2009) RIP3, an energy metabolism regulator that switches TNF-induced cell death from apoptosis to necrosis. *Science* **325,** 332–336 CrossRef Medline
25. He, S., Liang, Y., Shao, F., and Wang, X. (2011) Toll-like receptors activate programmed necrosis in macrophages through a receptor-interacting kinase-3-mediated pathway. *Proc. Natl. Acad. Sci. U.S.A.* **108,** 20054–20059 CrossRef Medline
26. Lin, J., Kumari, S., Kim, C., Van, T. M., Wachsmuth, L., Polykratis, A., and Pasparakis, M. (2016) RIPK1 counteracts ZBP1-mediated necroptosis to inhibit inflammation. *Nature* **540,** 124–128 CrossRef Medline
27. Newton, K., Wickliffe, K. E., Maltzman, A., Dugger, D. L., Strasser, A., Pham, V. C., Lill, J. R., Roose-Girma, M., Warming, S., Solon, M., Ngu, H., Webster, J. D., and Dixit, V. M. (2016) RIPK1 inhibits ZBP1-driven necroptosis during development. *Nature* **540,** 129–133 CrossRef Medline
28. Thapa, R. J., Ingram, J. P., Ragan, K. B., Nogusa, S., Boyd, D. F., Benitez, A. A., Sridharan, H., Kosoff, R., Shubina, M., Landsteiner, V. J., Andrake, M., Vogel, P., Sigal, L. J., ten Oever, B. R., Thomas, P. G., *et al.* (2016)DAIsensesinfluenzaAvirusgenomicRNAandactivatesRIPK3-dependent cell death. *Cell Host Microbe* **20,** 674–681 CrossRef Medline
29. Kaczmarek, A., Vandenabeele, P., and Krysko, D. V. (2013) Necroptosis: the release of damage-associated molecular patterns and its physiological relevance. *Immunity* **38,** 209–223 CrossRef Medline
30. Wang, X., Jiang, W., Yan, Y., Gong, T., Han, J., Tian, Z., and Zhou, R. (2014) RNA viruses promote activation of the NLRP3 inflammasome through a RIP1-RIP3-DRP1 signaling pathway. *Nat. Immunol.* **15,** 1126–1133 CrossRef Medline
31. Moriwaki, K., Bertin, J., Gough, P. J., and Chan, F. K. (2015) A RIPK3-caspase 8 complex mediates atypical pro-IL-1β processing. *J. Immunol.* **194,** 1938–1944 CrossRef
32. Najjar, M., Saleh, D., Zelic, M., Nogusa, S., Shah, S., Tai, A., Finger, J. N., Polykratis, A., Gough, P. J., Bertin, J., Whalen, M., Pasparakis, M., Balachandran, S., Kelliher, M., Poltorak, A., *et al.* (2016) RIPK1 and RIPK3 kinases promote cell-death-independent inflammation by Toll-like receptor 4. *Immunity* **45,** 46–59 CrossRef Medline
33. Kutuzova, G. D., Albrecht, R. M., Erickson, C. M., and Qureshi, N. (2001) Diphosphoryl lipid A from Rhodobacter sphaeroides blocks the binding and internalization of lipopolysaccharide in RAW 264.7 cells. *J. Immunol.* **167,** 482–489 Medline
34. Jarvis, B. W., Lichenstein, H., and Qureshi, N. (1997) Diphosphoryl lipid A from *Rhodobacter sphaeroides* inhibits complexes that form *in vitro* between lipopolysaccharide (LPS)-binding protein, soluble CD14, and spectrally pure LPS. *Infect. Immunol.* **65,** 3011–3016 Medline
35. Youn, J. H., Kwak, M. S., Wu, J., Kim, E. S., Ji, Y., Min, H. J., Yoo, J. H., Choi, J. E., Cho, H. S., and Shin, J. S. (2011) Identification of lipopolysaccharide-binding peptide regions within HMGB1 and their effects on subclinical endotoxemia in a mouse model. *Eur. J. Immunol.* **41,** 2753–2762 CrossRef Medline
36. Kim, S. J., and Li, J. (2013) Caspase blockade induces RIP3-mediated programmed necrosis in Toll-like receptor-activated microglia. *Cell Death Dis.* **4,** e716 CrossRef Medline
37. Kang, S., Fernandes-Alnemri, T., Rogers, C., Mayes, L., Wang, Y., Dillon, C., Roback, L., Kaiser, W., Oberst, A., Sagara, J., Fitzgerald, K. A., Green, D. R., Zhang, J., Mocarski, E. S., and Alnemri, E. S. (2015) Caspase-8 scaffolding function and MLKL regulate NLRP3 inflammasome activation downstream of TLR3. *Nat. Commun.* **6,** 7515 CrossRef Medline
38. Kaiser, W. J., Sridharan, H., Huang, C., Mandal, P., Upton, J. W., Gough, P. J., Sehon, C. A., Marquis, R. W., Bertin, J., and Mocarski, E. S. (2013) Toll-like receptor 3-mediated necrosis via TRIF, RIP3, and MLKL. *J. Biol. Chem.* **288,** 31268–31279 CrossRef Medline
39. Kayagaki, N., Warming, S., Lamkanfi, M., Vande Walle, L., Louie, S., Dong, J., Newton, K., Qu, Y., Liu, J., Heldens, S., Zhang, J., Lee, W. P., Roose-Girma, M., and Dixit, V. M. (2011) Non-canonical inflammasome activation targets caspase-11. *Nature* **479,** 117–121 CrossRef Medline
40. Broz, P., Ruby, T., Belhocine, K., Bouley, D. M., Kayagaki, N., Dixit, V. M., and Monack, D. M. (2012) Caspase-11 increases susceptibility to *Salmonella* infection in the absence of caspase-1. *Nature* **490,** 288–291 CrossRef Medline
41. Sun, L., Wang, H., Wang, Z., He, S., Chen, S., Liao, D., Wang, L., Yan, J., Liu, W., Lei, X., and Wang, X. (2012) Mixed lineage kinase domain-like protein mediates necrosis signaling downstream of RIP3 kinase. *Cell* **148,** 213–227 CrossRef Medline
42. Wang, H., Sun, L., Su, L., Rizo, J., Liu, L., Wang, L. F., Wang, F. S., and Wang, X. (2014) Mixed lineage kinase domain-like protein MLKL causes necrotic membrane disruption upon phosphorylation by RIP3. *Mol. Cell* **54,** 133–146 CrossRef Medline
43. Nogusa, S., Thapa, R. J., Dillon, C. P., Liedmann, S., THOguin 3rd, Ingram, J. P., Rodriguez, D. A., Kosoff, R., Sharma, S., Sturm, O., Verbist, K., Gough, P. J., Bertin, J., Hartmann, B. M., Sealfon, S. C., *et al.* (2016) RIPK3 activates parallel pathways of MLKL-driven necroptosis and FADD-mediated apoptosis to protect against influenza A virus. *Cell Host Microbe* **20,** 13–24 CrossRef Medline
44. Ito, Y., Ofengeim, D., Najafov, A., Das, S., Saberi, S., Li, Y., Hitomi, J., Zhu, H., Chen, H., Mayo, L., Geng, J., Amin, P., DeWitt, J. P., Mookhtiar, A. K., Florez, M., *et al.* (2016) RIPK1 mediates axonal degeneration by promoting inflammation and necroptosis in ALS. *Science* **353,** 603–608 CrossRef Medline
45. Zhang, T., Zhang, Y., Cui, M., Jin, L., Wang, Y., Lv, F., Liu, Y., Zheng, W., Shang, H., Zhang, J., Zhang, M., Wu, H., Guo, J., Zhang, X., Hu, X., *et al.* (2016) CaMKII is a RIP3 substrate mediating ischemia- and oxidative stress-induced myocardial necroptosis. *Nat. Med.* **22,** 175–182 CrossRef Medline
46. Newton, K., Dugger, D. L., Maltzman, A., Greve, J. M., Hedehus, M., Martin-McNulty, B., Carano, R. A., Cao, T. C., van Bruggen, N., Bernstein, L., Lee, W. P., Wu, X., DeVoss, J., Zhang, J., Jeet, S., *et al.* (2016) RIPK3 deficiency or catalytically inactive RIPK1 provides greater benefit than MLKL deficiency in mouse models of inflammation and tissue injury. *Cell Death Differ.* **23,** 1565–1576 CrossRef Medline
47. Daniels, B. P., Snyder, A. G., Olsen, T. M., Orozco, S., Oguin, T. H., 3rd, Tait, S. W. G., Martinez, J., Gale, M., Jr., Loo, Y. M., and Oberst, A. (2017) RIPK3 restricts viral pathogenesis via cell death-independent neuroinflammation. *Cell* **169,** 301–313.e311 CrossRef Medline
48. Meng, J., Drolet, J. R., Monks, B. G., and Golenbock, D. T. (2010) MD-2 residues tyrosine 42, arginine 69, aspartic acid 122, and leucine 125 provide species specificity for lipid IVA. *J. Biol. Chem.* **285,** 27935–27943 CrossRef Medline
49. Weng, D., Marty-Roix, R., Ganesan, S., Proulx, M. K., Vladimer, G. I., Kaiser, W. J., Mocarski, E. S., Pouliot, K., Chan, F. K., Kelliher, M. A.,

Harris, P. A., Bertin, J., Gough, P. J., Shayakhmetov, D. M., Goguen, J. D., *et al.* (2014) Caspase-8 and RIP kinases regulate bacteria-induced innate immune responses and cell death. *Proc. Natl. Acad. Sci. U.S.A.* **111,** 7391–7396 CrossRef Medline

50. Wang, Y., Gao, W., Shi, X., Ding, J., Liu, W., He, H., Wang, K., and Shao, F. (2017) Chemotherapy drugs induce pyroptosis through caspase-3 cleavage of a gasdermin. *Nature* **547,** 99–103 CrossRef Medline
51. Duarte, D. B., Vasko, M. R., and Fehrenbacher, J. C. (2016) Models of inflammation: carrageenan air pouch. *Curr. Protocols Pharmacol.* **72,** 5.6.1–9 Medline
52. Qu, Y., Tang, J., Wang, H., Li, S., Zhao, F., Zhang, L., Richard Lu, Q., and Mu, D. (2017) RIPK3 interactions with MLKL and CaMKII mediate oligodendrocytes death in the developing brain. *Cell Death Dis.* **8,** e2629 CrossRef Medline